Transparent broadband microwave metamaterial absorber with thermal insulating and soundproof*

YANG Chang (杨昌)[1,2], **CHEN Sai** (陈赛)[2,3]**, **NIU Shuai** (牛帅)[2], **XIAO Lin** (肖林)[2,3]**, and **QU Yan-chen** (曲彦臣)[1]**

1. *National Key Laboratory of Science and Technology on Tunable Laser, Harbin Institute of Technology, Harbin 150080, China*
2. *Nanophotonics and Optoelectronics Research Center, Qian Xuesen Laboratory of Space Technology, China Academy of Space Technology, Beijing 100094, China*
3. *Key Laboratory of Infrared Imaging Materials and Detectors, Shanghai Institute of Technical Physics, Chinese Academy of Sciences, Shanghai 200083, China*

(Received 15 February 2020; Revised 9 April 2020)

Nowadays, multi-functional materials are desperately required for adapting the complex environment, which urges us to take more factors into consideration. Here, we proposed a broadband microwave absorber with multi-functionality such as optically transparent, thermal insulating and soundproof properties. Using indium tin oxide (ITO) based metamaterial, the device can achieve above 90% microwave absorption from 5.6 GHz to 23 GHz (cover X and Ku band). Moreover, with designed vacuum structure inside, the device is thermal insulating and soundproof. These multi-functional advantages give the absorber more flexibility in electromagnetic shielding and stealth application, which can be potentially applied in windows related industry.

Document code: A **Article ID:** 1673-1905(2021)02-0085-5

DOI https://doi.org/10.1007/s11801-021-0023-8

Microwave broadband absorbers can dissipate the energy of electromagnetic (EM) wave into heat, eliminating the reflected wave along the echo direction or eliminating adverse EM wave radiation over a relatively wide frequency range. At present, microwave absorbers are largely applied to variant fields such as EM shielding and transparency, which can render objects undetectable by microwave[1] or reduce the EM pollution for healthcare[2,3] and electronic safety[4,5]. Most of conventional absorber has the disadvantage of being opaque, the drawback restricts their application in some scenarios requiring optical transparency and strong microwave absorption simultaneously[6-9].

In recent years, metamaterials have been applied into microwave absorbers[10-14]. By selecting appropriate parameters of structure, the effective permittivity and permeability can be manipulated and matching the impedance to free space[15-17]. Compared with material-based absorber[18-20], microwave metamaterial absorbers (MMA) can also be implemented to achieve high efficiency and broadband EM wave absorption[21–25]. For these MMAs, the mostly absorption comes from the intrinsic resonance of the structures. Moreover, it can be weaved by transparent conductive material, structures containing transparent spacers and ultrathin resistive layers like graphene, indium tin oxide (ITO), or other conducting oxides[25-28]. For example, Jang et al use polyethylene terephthalate (PET) and polydimethylsiloxane (PDMS) layer as the spacer, separating the small metallic pattern layer and mesh layer, which realizes absorptivity more than 90% from 5.8 GHz to 12.2 GHz[25]. However, for 8—18 GHz regime (X and Ku band), there are few reports to cover. Until recently, Zhang et al designed a transparent sandwich structure constructed by ITO, polymethyl methacrylate (PMMA) and PET, which realizes over 90% from 8.3 GHz to 17.4 GHz[26]. However, for current designs, the absorption mostly happens on the upper ITO structures of these MMAs which are always exposed to the environment. It is easily damaged or influenced by environment and losing function. Therefore, it is necessary to take this problem into consideration. Moreover, for the application on windows related field, the thermal control and soundproof are also important factors.

In this paper, we design an optically transparent MMA over a wide frequency band from 5.7 GHz to 23 GHz. The transparent and conducting material was used for

* This work has been supported by the Open Research Funding from Key Laboratory of Infrared Imaging Materials and Detectors (Shanghai Institute of Technical Physics, Chinese Academy of Sciences).
** E-mails: cescchen1990@gmail.com; xiaolin@qxslab.cn; quyanchen@hit.edu.cn

both basic absorption element and the back reflective layer. ITO is deposited on the inside of two quartz plates, which can prevent ITO from being damaged by exposure to the environment. The PVC film overs the outside of the upper quartz plate decrease the insert loss. The vacuum space is designed for separating the two quartz plates which can provide a sound and thermal isolation environment. With all these advantages, the absorber can broadly be applied as a kind of multi-functional window adapted to more complicated scenarios in electromagnetic shielding and stealth field essential for efficient review and publication of submissions.

The schematic of the proposed MMA is illustrated in Fig.1(a). From the top to bottom, the MMA consists of three layers. The top layer is an impedance matching layer for reducing the backward reflections. The middle-layer film is constructed by periodic-pattern-array ITO film used as a microwave resonator. The bottom-layer ITO film behaves as an EM reflective mirror layer. In order to provide thermal and sound isolation environment, the middle-layer ITO pattern and bottom-layer ITO film are coated on quartz substrates separated by a vacuum spacer. As shown in Fig.1(b), the typical unit cell consists of the PVC placed on the top of upper quartz substrate, the fan-blade-shaped ITO patterns and ITO film deposited on inside of the quartz substrates. The surface resistance of the ITO material for the pattern and bottom are 15 Ω/□ and 30 Ω/□, respectively. The dielectric constants of PVC and quartz are set as $\varepsilon_{pvc}=2.3(1-j0.001)$ and $\varepsilon_{quartz}=3.6(1-j0.01)$, respectively. The dimensions of the unit cells shown in Fig.1(b) and (c) are $d_{PVC}=1$ mm, $d_{SiO2}=2.3$ mm, $d_{vacuum}=2.2$ mm, $w_1=4$ mm, $w_2=1.1$ mm, $L_1=1.4$ mm, $L_2=2$ mm.

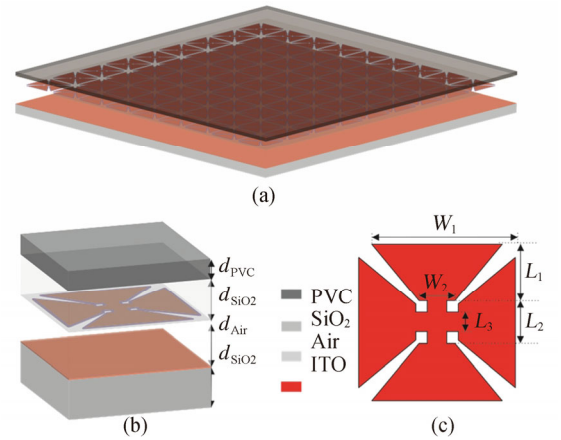

Fig.1 (a) Schematic of a broadband optically transparent microwave metamaterial absorber; (b) and (c) The geometry of the unit cell

Generally, the resonant structure possesses a high Q factor, which leads to narrow band reflection or absorption. To broaden absorption bandwidth, we design a fan-blade-shaped resonator. This pattern has two advantages: on the one hand, due to the symmetry of the pattern, the absorption performance is insensitive to the polarization of the incident wave; on the other hand, the fan-blade shape can provide multi-resonance, inducing the resonance coupling, which improves the bandwidth of the resonance. To demonstrate the characters of the absorber, we simulated the absorptivity spectra of the unit cell with normal incidence, where the polarization direction is set along *y*-axis. As shown in Fig.2(a), there is a broadband absorption from 5.5 GHz to 23 GHz with 90% upper absorption. There are three resonant absorption peaks in the curve, which locates at 6.6 GHz, 12.6 GHz and 20.9 GHz, respectively. Fig.2(b) displays the top view of the electrical field distribution of the metamaterial at the three absorption peak frequencies (f_1=6.6 GHz, f_2=12.6 GHz and f_3=20.9 GHz). The spoof surface plasmonic resonance region is enclosed by white dotted line. At 6.6 GHz, the electric field is strongly localized in the gap between the upper and lower fan blades. When the frequency is 20.9 GHz, the electric field is strongly localized around the edges of the fan blade. At 12.6 GHz, the two resonant modes mentioned above exist simultaneously, and a third resonance peak comes into being by coupling. Because of the three resonance peaks existing, the MMA realizes a broadband absorption from 5.7 GHz to 23 GHz.

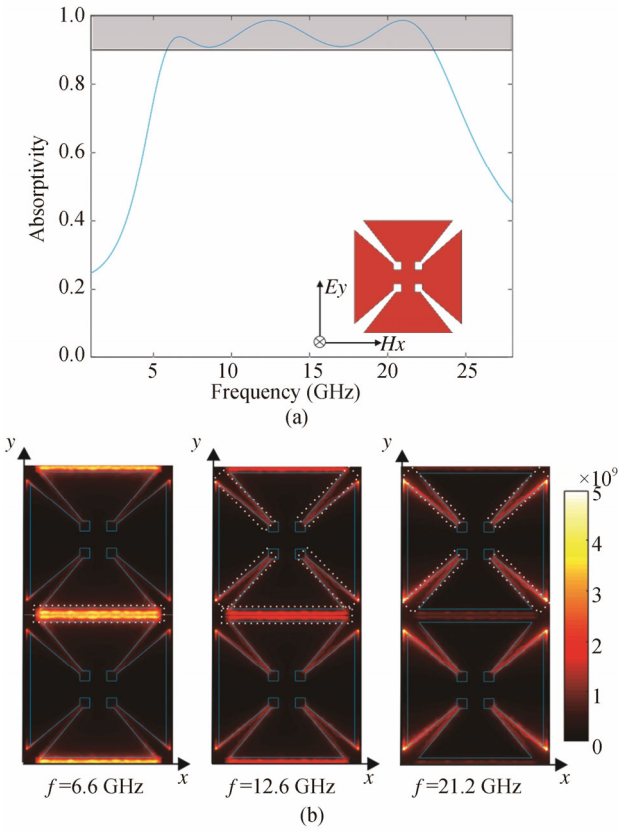

Fig.2 (a) Simulated absorptivity (1-*T*-*R*) of the structure (the inset) under the normal incidence (The electric field component is along the *Y*-axis.); (b) Electrical amplitude in the top view at 6.6 GHz,12.6 GHz and 21.2 GHz, respectively (The position of the white dotted line indicates a strong local area of energy.)

It is also significant to analyze the effect of adjusting the element geometry for absorption bandwidth and intensity. First, we change the two parameters, namely, the fan-blade length L_1 and width w_1 in Fig.1. We can observe the change of absorptivity from Figs.3(a) and (b), L_1 mainly affects the low-frequency part of absorption and w_1 mainly affects the high-frequency part of absorption. And then, we adjust the thicknesses of upper quartz and air space. As shown in the Figs.3(c) and (d), the whole absorption spectrum is red-shifted as the thickness increases, and the variety in d_{SiO2} affects the high frequency portion of absorption, whereas for d_{vacuum} the case is reverse.

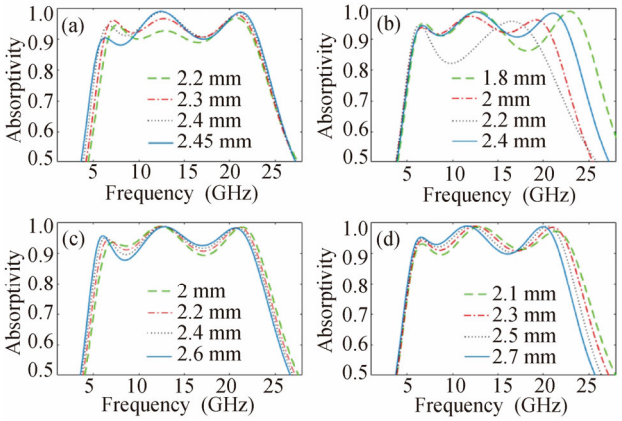

Fig.3 (a) and (b) Dependence of the simulated absorptivity on side length L_1 and linewidth w_1; (c) and (d) Dependence of the simulated absorptivity on thickness of d_{SiO2} and d_{vacuum}

Tab.1 summarizes the performance of the optically transparent microwave absorbers reported in recent years. By comparing these reports, our designed MMA has a better broadband microwave absorption capability. After realizing a wider microwave absorption range, the overall thickness of the structure remains relatively thin. Due to a vacuum layer was added to the typical sandwich structure[26,28], the MMA takes possession of blocking the transmission of sound and conduction of heat. At the same time, the thermal radiation is also overcome because of the existence of the EM back reflector layer. The MMA can provide a sound and thermal isolation environment.

Tab.1 Characteristics of the optically transparent microwave absorbers in the literatures

Absorber in references	Absorption bandwidth (GHz)	Thickness (mm)	Thermal and sound insulating
Ref.[21]	6–8; 12–18	5.5	No
Ref.[24]	6.1–14.7	5.0	No
Ref.[25]	5.8–12.2	4.9	No
Ref.[26]	8.3–17.4	3.5	No
Ref.[28]	8.0–15	2.55	No
Ref.[29]	8–18	4.6	No
This work	5.5–23	5.5	Yes

To design high efficiency electromagnetic wave MMA, for strong electromagnetic loss induced by the absorbing structure[29], impedance matching between the MMA and the free space is an important factor. As shown in Fig.4(a), we analyze the equivalent transmission line model of the designed MMA. Z_1 is the impedance of input impedance of the whole proposed MMA. Z_{ITO} is the impedance of the upper SiO_2 layer combining with the ITO pattern, Z_{pvc} and Z_d are the equivalent impedances of upper PVC and air, respectively. Z_0 is the impedance in vacuum. Z_1 is retrieved from the S-parameters of the unit cell according to the effective medium theory[30]. The retrieval equation is

$$Z_1 = \frac{\sqrt{(1+S_{11})^2 - S_{21}^2}}{\sqrt{(1-S_{11})^2 - S_{21}^2}} \quad . \tag{1}$$

The real and imaginary parts of the impedance Z_1 calculated by Eq.(1) are given in Fig.4(b). We can know that the real part of Z_1 (blue curve) is nearly 1 and the imaginary part (red curve) is nearly 0 from 5.7 GHz to 23 GHz. It is obvious that the MMA achieves impedance matching and minimizes the reflection from the MMA.

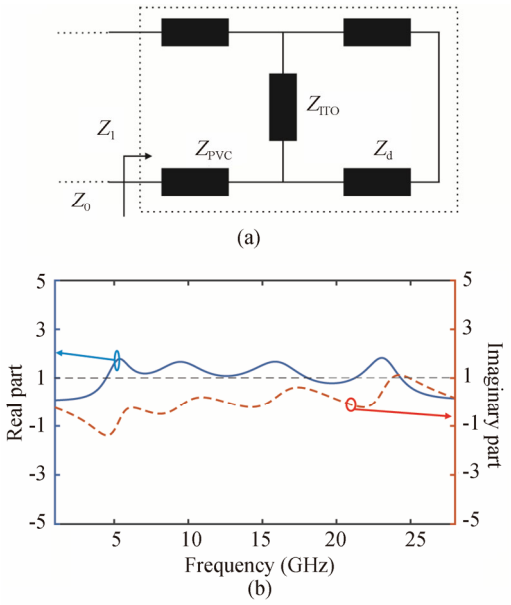

Fig.4 (a) Schematic of the equivalent TL model to retrieve the surface impedance of the MMA; (b) Impedances for Z_1: real part (blue curve) and imaginary part (red curves)

To analyze the contribution of each component of the MMA, we numerically simulate its absorptivity in case of absence of the PVC, ITO pattern, or ITO film, respectively. As shown in Fig.5(a), the absorptivity of the MMA without PVC is indicated by the magenta line. Compared with the black line in Fig.5(a), the absorption curvilinear as a whole decline and the absorptivity of below 90% emerges. It means the PVC film covers the outside of the upper quartz plate cannot only protect the structure, but plays a beneficial role in reduction of backward reflections.

As the blue line shows, the absorptivity is merely about 20%. It can be concluded that in the absence of fan-blade-shaped resonators, the MMA basically losts its ability to absorb microwaves, which proves that the absorption of the MMA is mainly caused by the fan-blade-shaped resonators.

When we extract ITO film from MMA, not only the bandwidth of absorption spectrum becomes narrow significantly but also the absorptivity dropped to 70%. Ground ITO film contribution to the broadband absorption can't be neglected. As shown in Fig.5(b), antiparallel surface currents are induced between the fan-blade-shaped resonators and ground ITO film. The directions of the induced surface current on the surface of the resonators lay and ground lay is indicated by yellow arrow and blue arrow, respectively. The simulated surface current distributions on two lays are shown in Fig.5(c) and (d). The antiparallel surface current let to mutually canceled magnetic fields, or strong absorption of the magnetic energy. Besides the localized surface plasmonic resonance of fan-blade-shaped resonators, the combination of the top and bottom ITO layers can influence the electromagnetic field, giving rise to significant energy dissipation by resistance of the resonators.

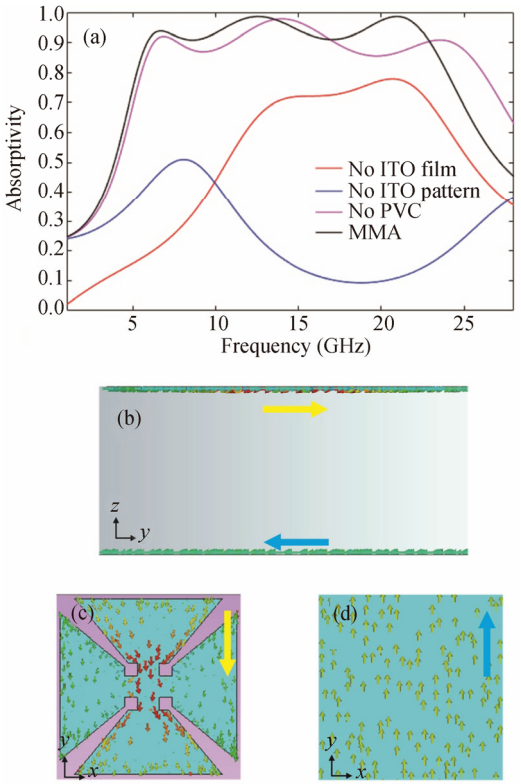

Fig.5 (a) Simulated results of the absorber with the absence of the upper PVC, middle resonator, and bottom ITO film, respectively; (b) Simulated surface current distributions of (c) the ITO-pattern resonator and (d) ITO film at 6.6 GHz under normal incidence

Besides, it is very important for MMA to maintain high microwave absorption efficiency during oblique incidence. The absorption characteristics of transverse electric polarization (TE) and transverse magnetic polarization (TM) of MMA at different incident angles were simulated, as shown in Fig.6. When the EM wave is normally incident, the absorption of both polarization modes by MMA is the same. In this case, MMA has the property of polarization independence. When the incident light comes in obliquely, the designed MMA can continue to be more than 90% absorption for TE/TM polarization when the incident angle is within 30°. When the incident Angle is greater than 30°, the performance of MMA deteriorated significantly. It is the result of mismatched impedance with oblique incidence. The MMA can still maintain 80% absorption within 45°. However, there is a little difference in the absorption performance between the TE and TM polarization. On the EM wave incident surface of MMA, for TE polarization, as the incident angle increases, the tangential component of magnetic field intensity decreases but the electric field remains unchanged. While for TM polarization, the characteristic is the opposite. Since the absorption is mainly localized electric field as discussed in Fig.2, TE polarization possesses relatively good microwave absorption properties than TM polarization. This conclusion is clearly proved in Fig.6(a) and (b). In short, for the oblique incidence of TE/TM polarized light, the MMA can both maintain more than 90% absorption. However, for the incident of TE polarization, the absorption performance is better.

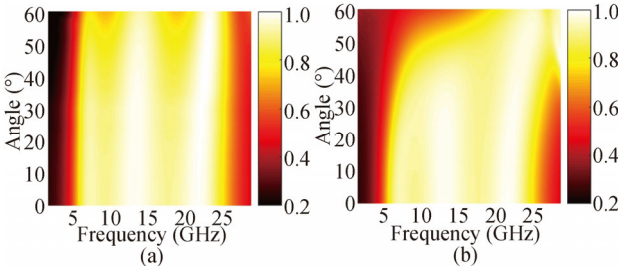

Fig.6 Simulated absorptivity spectra of the proposed MMA at incident angles from 0° to 70° for (a) TE and (b) TM waves

In summary, we have proposed a transparent and broadband MMA with thermal and sound insulating properties. As the result shows, the MMA realizes more than 90% total absorption with a wide frequency ranges from 5.7 GHz to 23 GHz. Owing to the use of materials with high transmittance in optical range, the MMA will not block the visible light. For TE and TM polarization, the MMA can maintain superior broadband absorption performance when the incident angle is less than 30°. At the same time, the MMA possesses the merit of not easily fatigue damaged, sound and thermal insulation. These characteristics provide an infinite prospect for microwave absorption detector, windows and other applications.

References

[1] W. H. Emerson, IEEE Trans. Antennas Propagation **21**, 484 (1973).

[2] F. Qin and C. Brosseau, J. Appl. Phys. **111**, 61301 (2012).

[3] X.W. Yin, L. Kong, L.T. Zhang, L.F. Cheng, N. Travitzky and P. Greil, Int. Mater. Rev. **59**, 326 (2014).

[4] D. Micheli, C. Apollo, R. Pastore and M. Marchetti, Compos. Sci. Technol. **70**, 400 (2010).

[5] W.Y. Duan, Q. Li, X.W. Yin, X.M. Liu, L.F. Cheng and L.T. Zhang, J. Eur. Ceram. Soc. **34**, 257 (2014).

[6] M. Grande, G.V. Bianco, M.A. Vincenti, D. de Ceglia, P. Capezzuto, V. Petruzzelli, M. Scalora, G. Bruno and A. D'Orazio, Opt. Express **24**, 22788 (2016).

[7] K. Takizawa and O. Hashimoto, IEEE Trans. Microwave Theory Tech. **47**, 1137 (1999).

[8] Y. Okano, S. Ogino and K. Ishikawa, IEEE Trans. Microwave Theory Tech. **60**, 2456 (2012).

[9] H. Kurihara, Y. Hirai, K. Takizawa, T. Iwata and O. Hashimoto, IEICE Trans. Electron. E88c, 2350 (2005).

[10] B. D. F. Casse, W. T. Lu, Y. J. Huang, E. Gultepe, L. Menon and S. Sridhar, Appl. Phys. Lett **96**, 023114 (2010).

[11] N. Liu, M. Mesch, T. Weiss, M. Hentschel and H. Giessen, Nano. Lett **10**, 2342 (2010).

[12] J. Hao, L. Zhou and M. Qiu, Phys. Rev. B **83**, 165107 (2011).

[13] Z. Wu, X. Q. Chen, Z. L. Zhang, L. Y. Heng, S. Wang and Y. H Zou, ACS Appl. Phys. Express **12**, 057003 (2019).

[14] J. Q. Zhang, X. Y. Wu, L. Y. Liu, C. Huang, X. Y. Chen, Z. Tian, C. M. OuYang, J. Q. Gu, X. Q. Zhang, M. X. He, J. G. Han, X. N. Luo and W. L. Zhang, Opt. Express **27,** 18 (2019).

[15] H. Tao, N. I. Landy, C. M. Bingham, X. Zhang, R. D. Averitt and W. J. Padilla, Opt. Express **16,** 7181 (2008).

[16] S. Bhattacharyya, S. Ghosh and K. V. Srivastava, J. Appl. Phys. **114**, 094514 (2013).F. Dincer, M. araaslan, E. nal and C. abah, Configuration. Prog. Electromagn. Res. **013**, 219 (2013).

[17] Y. Zhang, Y Huang and T. F. Zhang, Adv. Mater. **12**, 2049 (2015).

[18] M. S. Cao, J. Yang, W. L. Song, D. Q. Zhang, B. Wen, H. B. Jin, Z. L. Hou and J. Yuan, ACS Appl. Mater. Interfaces **4**, 6949 (2012).

[19] H. Chen, Z. Huang, Y. Huang, Y. Zhang, Z. Ge, B. Qin, Z. Liu, Q. Shi, P. Xiao, Y. Yang, T. Zhang and Y. Chen, Carbon **124**, 506 (2017).

[20] D.W. Hu, J. Cao, W. Li, C. Zhang, T. L. Wu, Q.F. Li, Z. H. Chen, Y. L. Wang and J. G. Guan, Adv. Opt. Mater. **5**, 1700109 (2017).

[21] Y. Zhang, J. P. Duan, B. Z. Zhang, W. D. Zhang and W. J. Wang, J. Alloy. Compd. **705**, 262 (2017).

[22] F. Yu, J. Wang, J. Wang, H. Ma, H. Du, Z. Xu and S. Qu, J. Appl. Phys. **119**, 134104 (2016).

[23] H. Sheokand, S. Ghosh, G. Singh, M. Saikia, K.V. Srivastava, J. Ramkumar and S.A. Ramakrishna, J. Appl. Phys. **122**, 105105 (2017).

[24] T. Jang, H. Youn, Y.J. Shin and L.J. Guo, ACS Photonics **1**, 279 (2014).

[25] C. Zhang, Q. Cheng, J. Yang, J. Zhao and T.J. Cui, Appl. Phys. Lett. **110**, 143511 (2017).

[26] Y. H Wu, J. J. Wang, S. F. Lai, X. B. Zhu and W. H. Gu, AIP Advance **9**, 025309 (2019).

[27] K. Chen, L. Cui, Y.J. Feng, J.M. Zhao, T. Jiang and B. Zhu, Opt. Express **25**, 5571 (2017).

[28] Q. Zhou, X.W. Yin, F. Ye, R. Mo, Z. M. Tang, X.M. Fan, L.F. Cheng and L.T. Zhang, Appl. Phys. A **125**, 131 (2019).

[29] X. D. Chen, B. I. Wu, J. A. Kong and T. M. Grzegorczyk, Phys. Rev. E **71**, 046610 (2005).